European Radiology (2018) 28:3943–3952
https://doi.org/10.1007/s00330-017-5294-x

MUSCULOSKELETAL

Vertebral metastases from neuroendocrine tumours: How to avoid false positives on ^{68}Ga-DOTA-TOC PET using CT pattern analysis?

Mathieu Gauthé[1,2] · Nathalie Testart Dardel[3] · Fernando Ruiz Santiago[4] · Jessica Ohnona[1,2] · Valérie Nataf[1,2] · Françoise Montravers[1,2] · Jean-Noël Talbot[1,2]

Received: 24 July 2017 / Revised: 8 December 2017 / Accepted: 27 December 2017 / Published online: 12 March 2018

Abstract

Objectives To develop criteria to improve discrimination between vertebral metastases from neuroendocrine tumours (NETs) and benign bone lesions on PET combined with CT using DOTA-D-Phe[1]-Tyr[3]-octreotide labelled with gallium-68 (^{68}Ga-DOTA-TOC).

Methods In 535 NET patients, ^{68}Ga-DOTA-TOC PET/CT examinations were reviewed retrospectively for vertebral CT lesions and/or PET foci. For each vertebral PET abnormality, appearance on CT, biological volume (BV), standardized uptake value (SUV_{max}) and ratios to those of reference organs were determined. All vertebral abnormalities were characterized as a metastasis, a typical vertebral haemangioma (VH) or other benign lesion.

Results In 79 patients (14.8 %), we found 107 metastases, 34 VHs and 31 other benign lesions in the spine. The optimal cut-off values to differentiate metastases from benign lesions were BV ≥0.72 cm^3, SUVmax ≥2, SUVmax ratio to a reference vertebra ≥2.1, to liver ≥0.28 and to spleen ≥0.14. They corresponded to lesion-based ^{68}Ga-DOTA-TOC PET/CT sensitivity of 87 %, 98 %, 97 %, 99 % and 94 %, and specificity of 55 %, 100 %, 90 %, 97 %, 100 %, respectively.

Conclusions The high sensitivity of ^{68}Ga-DOTA-TOC-PET/CT in detecting NET vertebral metastases was confirmed; this study showed that specificity could be improved by combining CT features and quantifying ^{68}Ga-DOTA-TOC uptake.

Key Points

- *Bone metastases in neuroendocrine tumours correlate with prognosis.*
- *Benign bone lesions may mimic metastases on ^{68}Ga-DOTA-TOC PET/CT imaging.*
- *The specific polka-dot CT pattern may be missing in some vertebral haemangiomas.*
- *Lesion atypical for haemangiomas can be better characterized by quantifying ^{68}Ga-DOTA-TOC uptake.*

Keywords Neuroendocrine tumours · Haemangioma · PET/CT · Incidental findings · Spinal neoplasms

Abbreviations

AUC	Area under the curve
BV	Biological volume
CT	Computed tomography
DOTA	1,4,7,10-tetraazacyclododecane-1,4,7,10-tetraacetic acid
DOTA-TOC	Edotreotide
FDG	^{18}F-fluorodeoxyglucose
^{68}Ga	Gallium-68
MRI	Magnetic resonance imaging
NET	Neuroendocrine tumour
NPV	Negative predictive value
OSEM	Ordered Subsets Expectation-Maximization
PET	Positron emission tomography
PPV	Positive predictive value
ROC	Receiver operating characteristic
RV	Reference vertebra
Se	Sensitivity
SOT	Standard of truth
Sp	Specificity
SR	Somatostatin receptor
SR-2	Somatostatin receptors subtype 2

✉ Mathieu Gauthé
mathieugauthe@yahoo.fr

[1] Médecine Nucléaire, Hôpital Tenon, 4 rue de la Chine, 75020 Paris, France

[2] Université P&M Curie, Paris, France

[3] Nuclear Medicine, CHU de Granada, Granada, Spain

[4] Radiology Department, CHU de Granada, Granada, Spain

SUV	Standardized uptake value
TOC	Tyr3-octreotide
VH	Vertebral haemangioma
VOI	Volume of interest

Introduction

Bone metastases of neuroendocrine tumours (NETs) are common (40 % in a post-mortem study [1]), and associated with poor survival [2, 3]. However, they are commonly missed on CT [4] and bone scintigraphy [5]. Somatostatin receptor (SR) positron emission tomography combined with computed tomography (PET/CT) shows a high uptake of the somatostatin analogue in the case of NET bone metastases due to the overexpression of somatostatin receptors [5–7]. The sensitivity (Se) of SR-PET/CT is markedly improved compared with the sensitivity of bone scintigraphy, SR scintigraphy or CT [4, 5, 8–10]. Putzer et al. [5] reported a 97 % Se for SR-PET/CT versus 58 % for CT in the same patients.

However, specificity (Sp) of SR-PET/CT might have been overestimated in earlier series, due to unexpected causes of false-positive findings that were described later. Indeed, benign bone lesions such as vertebral haemangiomas (VHs), which are usually asymptomatic and most frequently discovered as an incidental finding [11, 12], may show significant uptake on SR-PET/CT, as recently reported in a few isolated cases [13–16], and thus mimic metastases. The specific 'polka dot' pattern on CT allows the diagnosis of typical VHs, avoiding false-positive interpretation of vertebral metastases [17]. However, this pattern on CT is not present in all VHs.

The aim of this study was to evaluate the risk of misdiagnosing benign lesions as bone metastases in a large cohort of patients with NET referred for SR-PET/CT using DOTA-D-Phe^{1}-Tyr^{3}-octreotide labelled with gallium-68 (^{68}Ga-DOTA-TOC), and to improve the Sp by combining quantification of the ^{68}Ga-DOTA-TOC uptake by a lesion and its CT pattern.

Materials and methods

Population

Between February 2010 and March 2016, all patients were referred to our department for a proven or suspected NET. The ^{68}Ga-DOTA-TOC PET/CTs were performed either initially as part of a prospective study (Eudract N°2007-002610-19) or subsequently as a compassionate use authorized on an individual basis by the National Medicine Agency. ^{68}Ga-DOTA-TOC PET/CT examinations from all patients included in this cohort were retrospectively reviewed, to search for one or several vertebral abnormalities.

This study was approved by our institutional review board. All patients gave their written consent for the subsequent use of their PET/CT images for research purposes.

^{68}Ga-DOTA-TOC imaging

The somatostatin analogue ligand was the octreotide derivative DOTA-TOC labelled with ^{68}Ga, which shows a high affinity for the SR subtype 2 (SR-2).

^{68}Ga was eluted from a ^{68}Ge/^{68}Ga generator (GalliaPharm, Eckert & Ziegler Radiopharma GmBH, Berlin, Germany). DOTA-TOC was labelled with ^{68}Ga according to the manufacturer's instructions.

No preparation of the patient was required before the injection. Patients received 1-2 MBq/kg body mass of ^{68}Ga-DOTA-TOC, injected via an infusion line connected to saline. Image acquisition was started 60 min after injection. The PET/CT machine was a GEMINI TF 16, (Philips Medical Systems, Cleveland, OH, USA). The examination field extended from the vertex to the mid-thigh with an imaging time of 2 min per bed position. Low-dose CT without contrast-enhancement was performed prior to PET acquisition (120 kVp, 80 mAs, slice thickness 2.5 mm, pitch 0.813, rotation time 0.5 s, field of view (FOV) 600 mm) for attenuation correction and anatomic localization. PET images were acquired in 3D mode, with FOV 576 mm, matrix 144 × 144; images were reconstructed using the OSEM weighted method based on three iterations and 33 subsets.

Image analysis

Images were uploaded on a dedicated workstation (Syngo.via®, Siemens Healthcare, Erlangen, Germany). Readers were blinded to clinical and biological data.

Analysis was limited to the spine, from the cervical spine to the sacrum, on transaxial, coronal and sagittal slices, using bone windows for CT (width=1,500, level=300).

First a radiologist with 8 years of experience in reading spine CT analysed the CT scans, without access to PET images, in order to classify radiological abnormalities in the spine as: (1) Typical VH presenting the 'polka dot' sign in axial planes or 'corduroy' sign on sagittal images [12, 17, 18], (2) atypical or ambiguous images or (3) typical lesions of osteoarthritis [18]. Then the radiologist classified atypical or ambiguous images according to their morphology: well-defined osteolytic, ill-defined osteolytic or osteoblastic lesion. In case of osteolytic lesions, the presence of cortical destruction was noted.

Secondly a nuclear physician, with 7 years of experience in reading PET/CT and 3 years of experience in reading SR-PET/CT, looked for any focal lesions on ^{68}Ga-DOTA-TOC PET/CT, with the information from the CT reading by the radiologist. For each vertebral focus on PET or abnormality on CT, the biological volume (BV), standardized uptake value (SUV_{max}) and its ratio

to the SUV_{max} of a visually normal reference vertebra (RV), of the liver and of the spleen were determined. The BV of each vertebral focus included the voxels corresponding to the area of the vertebral lesion on CT with a SUV greater than 50 % of SUV_{max} in this area. RV SUV_{max} was measured on the body of a normal lumbar vertebra using a $1cm^3$ VOI; liver and spleen SUV_{max} were recorded using a $1cm^3$ VOI centred on normal parenchyma. BV and SUV_{max} values of each focus were determined automatically after a semiautomatic determination of the VOI by the nuclear physician who also noted its corresponding appearance on CT: as osteoblastic, osteolytic, typical VH or no visible lesion.

Standard of truth (SOT)

The SOT was determined by a medical panel only aware of the location of CT lesion and/or ^{68}Ga-DOTA-TOC foci, which were listed according to the reading of the radiologist and the nuclear physician, but not to their intensity of uptake and CT pattern. This panel aimed to characterize each vertebral abnormality as metastasis, typical VH or other benign lesion, according to a composite SOT based on lesion evolution during follow-up (increase, decrease or disappearance); response of the lesion to therapy targeting NET; typical features on CT and/or MRI and/or ^{18}F-DOPA PET/CT [19].

Statistical analysis

Data were analysed using SPSS Statistics software (IBM Corporation, Armonk, NY, USA). A *p*-value less than 0.05 was considered to be statistically significant.

The Gaussian distribution of PET parameters was tested using Kolmogorov-Smirnov and Shapiro-Wilk normality test.

Lesion-based comparisons of BV, SUV_{max}, SUV_{max} ratios to RV, to liver and to spleen were performed between the three groups, metastases, VHs or other benign vertebral lesions, using one-way ANOVA followed, in case of significance, by the post-hoc Fisher's PSLD test, adjusted for clustering. Another comparison between non-VH lesions according to their CT pattern (osteoblastic, osteolytic or non-visible) was performed similarly.

Receiver operating characteristic (ROC) analysis was used to determine area under the curve (AUC) and the optimal cut-off values for the different parameters quantifying ^{68}Ga-DOTA-TOC uptake, to discriminate between metastatic and non-malignant vertebral abnormalities. The patient-based analysis was derived as usual from the lesion-based analysis; the association of false-negative and false-positive results in a given patient was quoted as a false-positive patient-based result. Patient-based and lesion-based comparisons of sensitivity and specificity were performed using Chi-squared tests, according to CT pattern alone, PET parameters alone and combined PET/CT information.

Results

Patient characteristics

During the observation period, 535 patients had at least one ^{68}Ga-DOTA-TOC PET/CT scan in our department. According to blinded reading by the radiologist and then the nuclear physician, at least one vertebral abnormality was found in 80 patients. One patient was subsequently excluded from the analysis because of diffuse intense osteo-medullary ^{68}Ga-DOTA-TOC uptake, making lesion assessment impossible. The mean follow-up duration after ^{68}Ga-DOTA-TOC-PET/CT was 36 months (range: 13–83).

Among the 79 remaining patients, at least one typical vertebral VH was identified on CT by the radiologist in 28 patients (5.2 % of the whole cohort of patients with NET), who had a total of 34 vertebral VHs. Twenty-two patients had one and six had two VHs. Sixteen VHs (47 %) were found in males and 18 (53 %) in females. Twenty-one VHs (62 %) were detected in the thoracic spine and 13 (38 %) in the lumbar spine. The most commonly affected vertebra was L1 (15 % of the VH). None of the 28 patients with VH presented with ambiguous vertebral lesions or bone metastases.

Apart from typical VH, at least one vertebral anomaly was found in 51 patients (9.7 % of the whole cohort of patients with NET). A total of 138 vertebral anomalies were detected in this non-VH group. The most frequently affected site was the thoracic spine (68/138), followed by the lumbar (40/138), the cervical (19/138) and the sacral (11/138) segments.

Ten patients had splenectomy (13 %) and 23 (29 %) had liver metastases.

Follow-up data over at least 2 years were available for 69/79 patients. In the 10/79 patients whose follow-up was available for less than 2 years: lesions progressed clearly in five patients and were considered to be metastases; in four patients, the lesions had the typical pattern of a VH on CT; in one patient, the lesion was characterized as a benign bone island on MRI. All other lesions that showed no change on imaging modalities over more than 2 years were considered to be benign. Thus, according to the SOT, 24 of the 51 patients of the non-VH group had at least one vertebral metastasis (Table 1). The total number of vertebral metastases was 107, among which 73 were osteoblastic, nine were osteolytic and 25 had no corresponding lesion on CT (Table 2). Metastatic and benign vertebral lesions were seen together in four patients. Twenty-seven patients of the non-VH group had no vertebral metastases. A total of 31 benign vertebral lesions were found in the non-VH group, of which six were osteoblastic, six were diagnosed as bone islands and 25 were osteolytic. The osteolytic lesions consisted in 12 non-typical VHs, five simple bone cysts (one an intraspongious hernia) and seven that remained of an undetermined aetiology but of benign nature, according to the SOT. Thus, benign vertebral lesions mainly appeared as well-defined and osteolytic, and metastases were

Table 1 Patient characteristics

Patient characteristics	With vertebral metastases	Without vertebral metastases
n	24	55
Gender (male/female)	13/11	27/28
Median age	69 ± 15 years (range: 30-93)	59 ± 13 years (range: 27-90)
18-39 y.o.	3 (12%)	5 (9%)
40-59 y.o.	5 (21%)	26 (47%)
> 60 y.o.	16 (67%)	24 (44%)
Primary NET		
Lung	7 (29%)	9 (16%)
Pancreas	6 (25%)	25 (45%)
Other	5 (21%)	14 (26%)
Unknown	6 (25%)	7 (13%)
PET/CT indications		
Search for primary NET	5 (21%)	9 (16%)
Lesion characterization	0 (0%)	9 (16%)
Initial workup	4 (17%)	14 (26%)
Monitoring	13 (54%)	16 (29%)
Recurrence workup	2 (8%)	7 (13%)
Ongoing medical treatment	8 (33%)	9 (16%)
lanreotide	6	7
everolimus	2	2

mainly osteoblastic or without corresponding lesion on CT (Chi^2=72; p<0.01).

None of the 26 osteolytic benign vertebral lesions presented with cortical destruction on CT, whereas it was seen in 7/10 osteolytic metastases.

^{68}Ga-DOTA-TOC detection rate and uptake

Visually, all NET metastases and all VHs were detected as foci on ^{68}Ga-DOTA-TOC PET/CT, while only 19/31 (61 %) of other benign lesions were visualized on PET.

The mean SUV_{max} of the reference organs was 8.1 (95 % CI: 7.7–8.6), 22.0 (95 % CI: 20.6–23.7) and 0.88 (95 % CI: 0.82–0.93) the reference being liver, spleen or RV, respectively. Because of a large hepatic involvement, measurement of the SUV_{max} of the liver was difficult in 7/23 patients with liver metastases (but was considered as feasible by the blinded reader).

The distribution of the raw SUVmax values significantly differed from the Gaussian model; thus, a logarithmic transformation was applied, resulting in a Gaussian distribution that enables the use of the parametric tests for comparison, as scheduled.

VHs and non-VH lesions had significantly greater mean SUV_{max} than RVs (p<0.001). Mean BV, SUV_{max} and SUV_{max} ratios were significantly greater for metastases than for VHs or

Table 2 Comparison of CT appearances between benign lesions and metastases

	Benign lesions	Metastases
n	65	107
Osteolytic	25 (39%)	10 (9%)
Well-defined	25	1 (none with cortical destruction)
Ill-defined osteolytic	0	9 (7 with cortical destruction)
Osteoblastic	6 (9%)	72 (67%)
Polka-dot CT pattern	34 (52%)	–
PET foci without corresponding lesion on CT	–	25 (24%)

Table 3 Lesion-based analysis comparing typical vertebral haemangiomas (VHs), other benign vertebral lesions and metastases, for parameters quantifying ^{68}Ga-DOTA-TOC uptake: SUVmax, SUVmax ratios to reference vertebra (RV), liver and spleen and biological volume (BV)

	VHs	Non-VHs		
	$n = 34$	Benign lesions $n = 31$	Metastases $n = 107$	ANOVA
SUV_{max}	2.2 [1.1-8.0]	1.0 [0.3-1.9]	8.7 [1.1-23.4]	$F = 48$; $p < 0.001$
VHs	–	$p = 0.3$	$p < 0.001$	
Benign lesions	$p = 0.3$	–	$p < 0.001$	
Metastases	$p < 0.001$	$p < 0.001$	–	
SUV_{max} ratio to RV	2.6 [1.2-8.4]	1.5 [0.4-3.8]	11.0 [1.7-56.2]	$F = 35$; $p < 0.001$
VHs	–	$p = 0.5$	$p < 0.001$	
Benign lesions	$p = 0.5$	–	$p < 0.001$	
Metastases	$p < 0.001$	$p < 0.001$	–	
SUV_{max} ratio to liver	0.31 [0.11-1.06]	0.15 [0.03-0.66]	1.18 [1.02-4.61]	$F = 41$: $p < 0.001$
VHs	–	$p = 0.335$	$p < 0.001$	
Benign lesions	$p = 0.335$	–	$p < 0.001$	
Metastases	$p < 0.001$	$p < 0.001$	–	
SUV_{max} ratio to spleen	0.08 [0.04-0.25]	0.04 [0.01-0.14]	0.49 [0.09-1.71]	$F = 45$; $p < 0.001$
VHs	–	$p = 0.6$	$p < 0.001$	
Benign lesions	$p = 0.6$	–	$p < 0.001$	
Metastases	$p < 0.001$	$p < 0.001$	–	
BV (cm^3)	3.7 [0.5-14.0]	0.9 [0.1-3.0]	1.9 [0.1-19.7]	$F = 15$; $p < 0.001$
VHs	–	$p < 0.001$	$p < 0.001$	
Benign lesions	$p < 0.001$	–	$p = 0.02$	
Metastases	$p < 0.001$	$p = 0.02$	–	

benign vertebral lesions, but their ranges overlapped (Table 3). No statistical differences were found between VHs and other benign lesions, except for BV, which was greater for VHs than for other benign lesion and for metastases (Table 3).

Considering the non-VH group, osteoblastic and non-visible lesions on CT corresponded on PET to foci with a significantly higher uptake than osteolytic lesions (respective mean ±SD: 9.0±6.4, 7.0±4.9 and 3.1±3.6; $p<0.001$), but the SUV_{max} of osteoblastic lesions did not significantly differ from that of non-visible lesions on CT ($p=0.2$).

Use of DOTA-TOC semi-quantification and of the CT pattern to characterize vertebral bone abnormalities

The optimal cut-off values determined by ROC analysis to distinguish vertebral metastases versus benign abnormalities were BV=0.72 cm^3 (AUC=0.47 (95 % CI: 0.37–0.58]), SUV_{max}=2 (AUC=0.97 (95 % CI: 0.95–1)), SUV_{max} ratio to RV=2.1 (AUC=0.59 (95 % CI: 0.50–0.68)]), SUV_{max} ratio to liver=0.28 (AUC=0.95 (95 % CI: 0.92–0.99)), SUV_{max} ratio to spleen=0.14 (AUC=0.98 (95 % CI: 0.97–1)) (Figs. 1, 2 and 3), and CT osteoblastic pattern (AUC=0.79 (95 % CI: 0.72–0.86)). Table 4 summarizes the diagnostic performance using above-defined cut-off values to characterize vertebral foci by using quantified PET information alone, CT pattern alone and quantified PET combined to identification of typical VH on CT.

The BV was the worst PET parameter for this differential diagnosis, with the sensitivity and specificity statistically inferior to those of SUV_{max} and SUV_{max} ratios in both patient and lesion-based analyses ($p<0.01$ for sensitivity and <0.001 for specificity, respectively). No statistical differences were found in performance between the other PET parameters. Finally, the SUV_{max} appeared to be the best PET parameter in practice because it could easily be evaluated in every situation, even in case of splenectomy or liver metastases.

On the patient-based analysis, SUV_{max} had a sensitivity of 96 %, statistically greater than 63 % for lesion pattern on CT ($p<0.0001$). On the other hand, CT pattern had a specificity of 91 %, non-significantly greater than 78 % for SUV_{max} ($p=0.09$). By combining the SUV_{max} and CT pattern, a sensitivity of 96 % was found (at least one lesion with $SUV_{max} \geq 2$ and no typical VH pattern on CT), statistically superior to that of CT pattern alone ($p<0.0001$). The corresponding specificity was 100% (all lesions with $SUV_{max} < 2$ or with typical VH

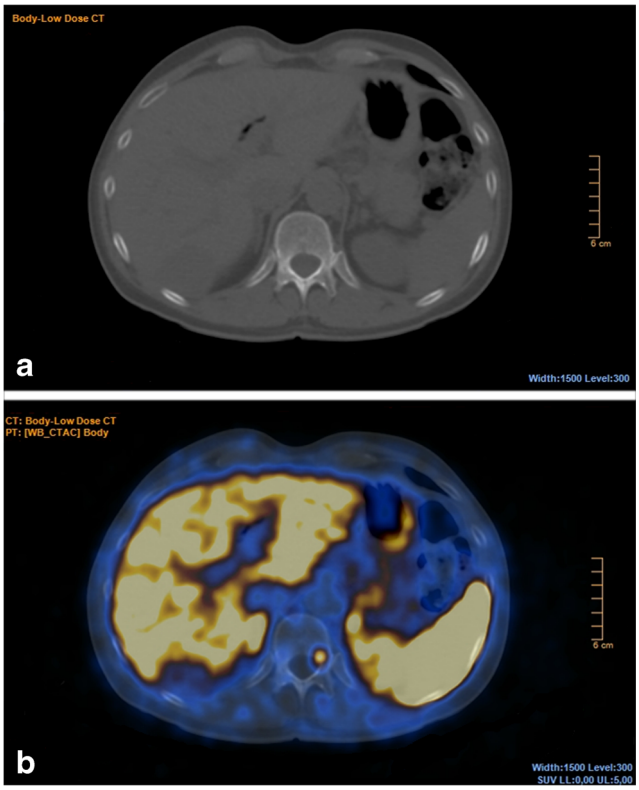

Fig. 1 Axial CT and fusion images centred on a vertebral metastasis of T12 demonstrating an intense DOTA-TOC uptake (SUV_{max}=6.5, SUV_{max} ratio to reference vertebra=5.6, to liver=0.92, to spleen=0.22) but without a corresponding lesion on CT, in a 58-year-old man referred for recurrence workup of a pancreatic neuroendocrine tumour (NET)

pattern on CT), statistically superior to both CT pattern alone and SUV_{max} alone (p=0.04 and 0.0002 respectively).

On the lesion-based analysis, SUV_{max} had a sensitivity of 98 %, statistically greater than 67 % for CT pattern (p=0.01). The CT pattern had a somewhat better specificity of 91 %, not significantly superior to 79 % for SUV_{max} (p=0.11). By combining the SUV_{max} and CT pattern, a sensitivity of 98 % was reached ($SUV_{max} \geq 2$ and no typical VH pattern on CT), statistically superior to that of CT pattern alone (p<0.01). The corresponding specificity was 100 % ($SUV_{max} < 2$ or with typical CT pattern on CT), statistically superior to both CT pattern alone and SUV_{max} alone (p=0.07 and 0.0008, respectively).

Discussion

Our study confirms the high sensitivity of ^{68}Ga-DOTA-TOC PET, being statistically superior to that of CT. This difference corresponds to bone metastases of NET which are not visible on CT (25/107=23 % lesion-based). This superiority has already been reported by Putzer et al. [5] in 51 NET patients: patient-based Se was 97 % for PET versus 58 % for CT, and Sp was 92 % for PET versus 100 % for CT.

By combining quantification of uptake on PET (SUV_{max}) and the search for VH pattern on CT, specificity increased up to 100 % and was statistically superior to specificity of quantified PET or CT pattern when considered separately. Ambrosini et al. [8] performed PET/CT using ^{68}Ga-DOTA-NOC in 223 NET patients; they reported that more bone metastases were detected on PET/CT when compared to CT in 20/35 patients, resulting in a higher patient-based sensitivity (100 % vs. 80 %) and specificity (100 % vs. 98 %).

This intense uptake of ^{68}Ga-DOTA-TOC by bone metastases is probably due to the persisting overexpression of the SR by those distant lesions, reflecting their differentiation. In some cases, dedifferentiation of metastases may occur and their affinity to somatostatin ligand may differ from that of the primary lesion, responsible for the failure of somatostatin analogue therapy [20, 21].

Concerning non-malignant lesions, all typical VHs on CT corresponded visually to ^{68}Ga-DOTA-TOC foci (Fig. 4). To

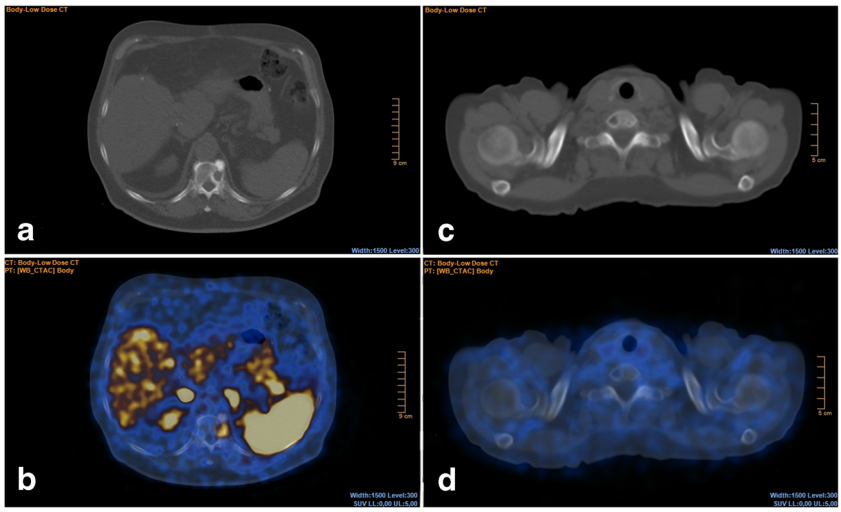

Fig. 2 Axial CT and fusion images. An osteolytic vertebral metastasis of T11 in a 72-year-old man referred for restaging of a lung neuroendocrine tumour (NET) showed an intense DOTA-TOC uptake (SUV_{max}=7.3, SUV_{max} ratio to reference vertebra=6.4, to liver=1.34, to spleen=0.26) (A and B). An osteolytic pure bone cyst of C7 in a 79-year-old woman referred for initial workup of a pancreatic NET showed no significant DOTA-TOC uptake (C and D)

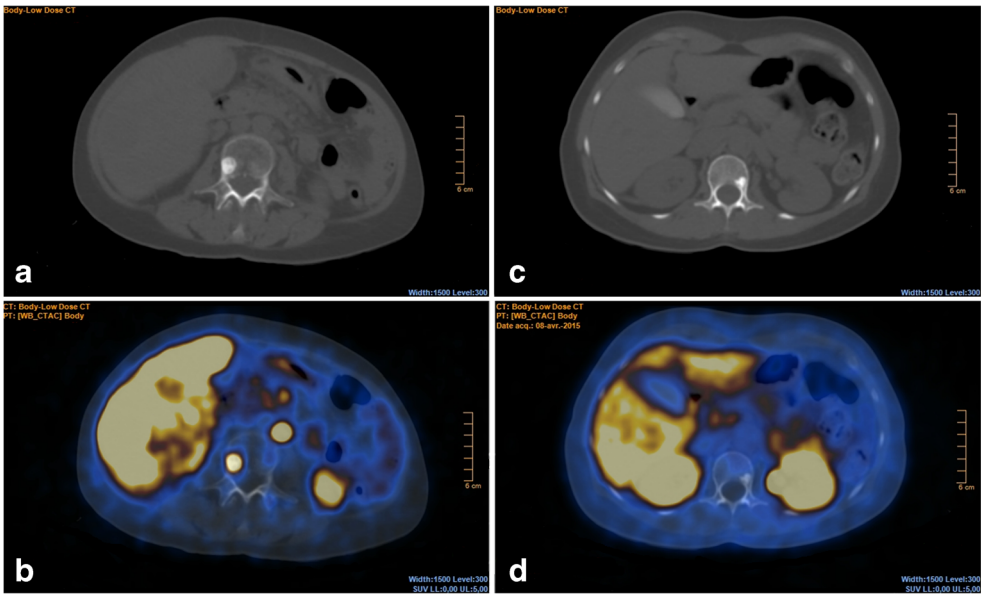

Fig. 3 Axial CT and fusion images. An osteoblastic vertebral metastasis of L3 in a 57-year-old woman referred for restaging of a lung neuroendocrine tumour (NET) showed an intense DOTA-TOC uptake (SUV_{max}=11.0, SUV_{max} ratio to reference vertebra=23.9, to liver=2.20, to spleen=0.72) (A and B). An osteoblastic bone island of L1 in a 54-year-old woman referred for characterization of a pancreatic lesion showed no significant DOTA-TOC uptake (C and D)

the best of our knowledge, only case reports of SR-PET radiotracer uptake in VHs have been previously published, as a potential pitfall in interpretation [13–16]. Indeed, identification of VH on CT [11, 12] is based on the 'polka-dot' pattern

Table 4 ^{68}Ga-DOTA-TOC PET/CT performance to characterize vertebral foci and/or CT abnormalities as malignant, excluding those presenting with a typical vertebral haemangioma (VH) pattern on CT, using aspect on CT or uptake quantification with cut-off values determined by receiver operating characteristic (ROC) analysis

	Cut-off	Se	Sp	PPV	NPV	Accuracy
Patient-based analysis						
CT pattern	Osteoblastic	63% (15/24)	91% (50/55)	75% (15/20)	85% (50/59)	82% (65/79)
PET parameter						
BV (cm^3)	≥ 0.72	75% (18/24)	29% (16/55)	32% (18/57)	73% (16/22)	43% (34/79)
SUV_{max}	≥ 2	96% (23/24)	78% (43/55)	66% (23/35)	98% (43/44)	84% (66/79)
SUV_{max} ratio						
To RV	≥ 2.1	96% (23/24)	67% (37/55)	56% (23/41)	97% (37/38)	76% (60/79)
To liver	≥ 0.28	100% (24/24)	82% (45/55)	71% (24/34)	100% (45/45)	87% (69/79)
To spleen	≥ 0.14	100% (21/21)	92% (44/48)	84% (21/25)	100% (44/44)	94% (65/69)
PET + CT	SUV_{max} ≥ 2 and no typical VH pattern on CT	96% (23/24)	100% (55/55)	100% (23/23)	98% (55/56)	99% (78/79)
Lesion-based analysis						
CT pattern	Osteoblastic	67% (72/107)	91% (59/65)	92% (72/78)	63% (59/94)	76% (131/172)
PET parameter						
BV (cm^3)	≥ 0.72	87% (93/107)	28% (18/65)	66% (93/140)	56% (18/32)	65% (111/172)
SUV_{max}	≥ 2	98% (105/107)	79% (51/65)	88% (105/119)	96% (51/53)	91% (156/172)
SUV_{max} ratio						
To RV	≥ 2.1	97% (104/107)	71% (46/65)	85% (104/123)	94% (46/49)	87% (150/172)
To liver	≥ 0.28	99% (106/107)	82% (53/65)	90% (106/118)	98% (53/54)	92% (159/172)
To spleen	≥ 0.14	94% (96/102)	93% (53/57)	96% (96/100)	90% (53/59)	94% (149/159)
PET + CT	SUV_{max} ≥ 2 and no typical VH pattern on CT	98% (105/107)	100% (65/65)	100% (105/105)	97% (65/67)	99% (170/172)

RV: reference vertebra; BV: biological volume; AUC: area under curve; Se: sensitivity; Sp: specificity; PPV: positive predictive value; NPV: negative predictive value

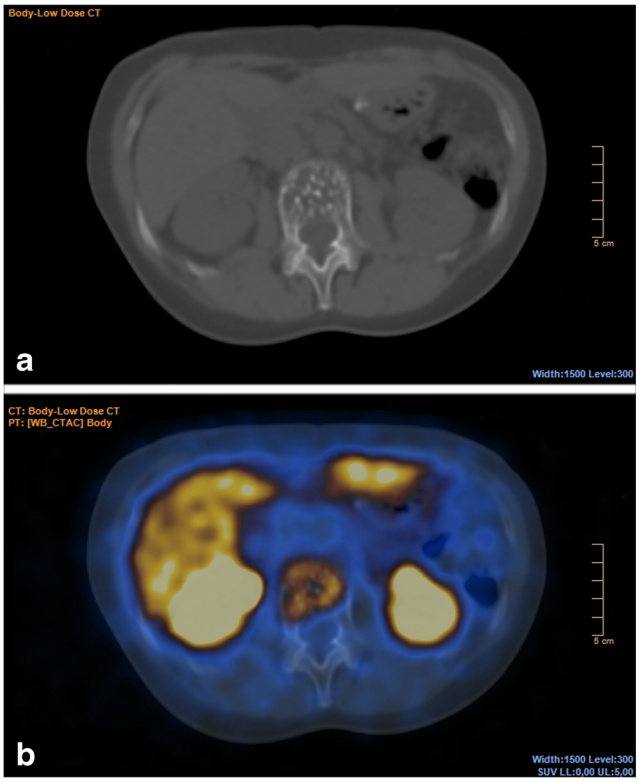

Fig. 4 Axial CT and fusion images centred on a typical vertebral haemangioma of L2 showing an intense DOTA-TOC uptake (SUV_{max}=8.0, SUV_{max} ratio to reference vertebra=8.4, to liver=0.49, to spleen=0.17) and the 'polka dot' pattern on CT, in a 60-year-old woman referred for initial workup of a pancreatic neuroendocrine tumour (NET)

in axial slices [12], which reflects the thickened trabeculae within the medullar cavity of the vertebral body [11]. Haemangiomas are benign vascular tumours composed of large cavernous spaces containing blood cells lined with a layer of flat endothelium [22]. Growing vascular endothelial cells expresses SR-2 [23]. Then it could be hypothesized that greater ^{68}Ga-DOTA-TOC uptake in VH compared to RV could be due to this benign endothelial proliferation. In contrast, VHs usually appeared as cold defects when other radiopharmaceuticals were used, as described on bone scintigraphy [24] and more recently on PET with ^{18}F-fluorodeoxyglucose (FDG) [25, 26] or ^{18}F-fluorocholine [27]. Although FDG uptake by one proven VH has been reported [28], SR ligands seem to be the only radiopharmaceuticals that are constantly taken-up by typical VH.

Concerning the benign lesions without the typical VH pattern on CT in the present study, 18 did not take-up ^{68}Ga-DOTA-TOC, as they probably did not overexpress SR. In contrast, 13 did show a greater ^{68}Ga-DOTA-TOC uptake than that of surrounding tissue: one intraspongious hernia that may have induced inflammatory hyperaemia, nine atypical haemangiomas characterized as such on MRI the uptake mechanism of which was discussed above, and 3 which remained unexplained but might be atypical haemangiomas that cannot be recognized with CT and MRI.

The added value of SR-PET to CT for assessing NETs has already been reported [29]. Actually the CT pattern may also help in discriminating vertebral lesions as benign or malignant: a high prevalence of the osteoblastic type in NET metastases was observed in our series, as previously reported by others [30]. Using the osteoblastic CT pattern as a criterion for malignancy, we found an accuracy of 82 % and 76 % in patient-based or lesion-based-analyses respectively.

As the most frequent site for bone metastases from a NET is the axial skeleton [5, 31], characterization of ambiguous vertebral lesions on CT as typical VH, osteoblastic, osteolytic with or without cortical rupture, or non-visible was thus of importance for a correct interpretation.

BV was not accurate for differentiating metastases from benign lesions. The FDG metabolic tumour volume was significantly correlated with outcome of various malignancies [32, 33], but this approach has not been validated using a biologic tracer such as ^{68}Ga-DOTA-TOC. In this context, it is not excluded that another threshold than 50% for BV determination could yield better diagnostic performance.

In our series, SUV_{max} appeared to be the easiest parameter to use in clinical practice in characterizing lesions as malignant or benign, with a statistically better sensitivity than CT pattern but with a potential loss of specificity. A greater mean SUV_{max} of ^{68}Ga-DOTA-TOC was reported by Kroiss et al. in 89 bone metastases of NET (19.8±18.8 vs. 8.7±5.8 in our series; Welsh's t-test $p<0.001$) but this difference disappeared when considering SUV_{max} ratio to RV (10.5±14.2 vs. 11±8.6 in our series Welsh's t-test $p=0.7$) [6]. Furthermore, mean SUV_{max} was similar to that reported with ^{68}Ga-DOTA-NOC by Prasad et al. on 78 bone metastases (mean SUV_{max} of 9.5 ±6 vs. 8.7±5.8 in our series; Welsh's t-test $p=0.5$) [7].

As an absolute value of SUV_{max} may slightly vary from one PET/CT machine to another, it might be recommended to use a SUV_{max} ratio to a reference organ. The choice of a reference vertebra did not lead to better results compared with using the liver or the spleen as reference organ. However, liver as a reference organ presented the drawback of a potential NET invasion which was detected in more than half of the NET patients with bone metastases [31, 34] and a non-negligible proportion of patients underwent splenectomy.

Limitations

Obtaining a histopathological evidence for asymptomatic and possibly benign lesions was ethically questionable and hardly feasible in practice. We thus accepted the typical pattern on CT as characterizing VHs. Similarly, the diagnosis of NET metastases and the characterization of ambiguous lesions as benign was based on a medical consensus derived from all available follow-up data, as none of the patients in this subset of patients was lost to follow-up. It was therefore not possible to formally characterize the actual nature of seven benign

vertebral lesions without a typical pattern on CT, which may be partly due to our choice of performing low-dose CT for PET/CT imaging.

Another potential limitation of this study was the retrospective analysis of the gathered data. However, examinations were acquired prospectively, with a similar technique and the same PET/CT machine and without any significant change in the imaging protocol over the time frame.

Another limitation was the fact we had to determine the cut-off values of ^{68}Ga-DOTA-TOC uptake to differentiate between vertebral metastases and benign lesions in this series. Therefore, the values of diagnostic performance derived from the same series using those cut-off values were only indicative and potentially overestimated.

In our study, only one radiologist and one nuclear physician reviewed the PET/CTs instead of two specialists for each modality. However, since the aim was neither to compare the agreement between readings nor to compare the clinical performance of the two imaging modalities, it did not appear worthwhile to recruit two other readers for the blinded reading of the 535 scans.

Finally, as our aim was to find ^{68}Ga-DOTA-TOC PET/CT criteria helping to characterize ambiguous vertebral SR-positive foci, the SOT was determined only for the 79 of 535 patients who had vertebral foci on PET and/or lesions on CT, but not for the whole series of patients. It was obviously possible that some patients will develop vertebral metastases during the subsequent evolution of their NET.

Conclusion

This study confirmed the high sensitivity of ^{68}Ga-DOTA-TOC PET in detecting vertebral metastases from NET. Benign lesions like VHs with typical radiological patterns had a ^{68}Ga-DOTA-TOC uptake higher than the normal appearing vertebrae, which may lead to false-positive results. This pitfall may be avoided by an accurate reading of the low dose CT of PET/CT, in search for typical VH pattern and also for an osteolytic pattern which appeared to be rare in case of NET metastasis, apart from cortical rupture or ill-defined limits of the lesion. Thus, combined reading of PET and CT increased the specificity of both modalities and lead to a diagnostic accuracy of 99 %.

Acknowledgements This study includes the data of a 'Projet de recherche clinique' PHRC P040303 sponsored by Assistance Publique-Hôpitaux de Paris monitored by Mrs Zakia Idir. We acknowledge the help of the Cancer Est Clinical Research Assistants during the clinical trial. We thank the referring physicians for their confidence and the medical technologists of our department for their commitment to PET/CT imaging. We thank Professor Ralph McCready for his assistance with editing the manuscript.

Funding The authors state that this retrospective analysis of data of a prospective series has not received any funding.

Compliance with ethical standards

Guarantor The scientific guarantor of this publication is Prof. J.N. Talbot.

Conflict of interest The authors of this manuscript declare no relationships with any companies whose products or services may be related to the subject matter of the article.

Statistics and biometry One of the authors has significant statistical expertise.

No complex statistical methods were necessary for this paper.

Informed consent Written informed consent was obtained from all subjects (patients) in this study.

Ethical approval Institutional Review Board approval was obtained.

Methodology
- retrospective
- diagnostic study
- performed at one institution

References

1. Ross EM, Roberts WC (1985) The carcinoid syndrome: comparison of 21 necropsy subjects with carcinoid heart disease to 15 necropsy subjects without carcinoid heart disease. Am J Med 79:339–354
2. Panzuto F, Nasoni S, Falconi M et al (2005) Prognostic factors and survival in endocrine tumor patients: comparison between gastrointestinal and pancreatic localization. Endocr Relat Cancer 12:1083–1092
3. Skoura E, Michopoulou S, Mohmaduvesh M et al (2016) The impact of 68Ga-DOTATATE PET/CT imaging on management of patients with neuroendocrine tumors: experience from a national referral center in the United Kingdom. J Nucl Med 57:34–40
4. Albanus DR, Apitzsch J, Erdem Z et al (2015) Clinical value of ^{68}Ga-DOTATATE-PET/CT compared to stand-alone contrast enhanced CT for the detection of extra-hepatic metastases in patients with neuroendocrine tumours (NET). Eur J Radiol 84:1866–1872
5. Putzer D, Gabriel M, Henninger B et al (2009) Bone metastases in patients with neuroendocrine tumor: 68Ga-DOTA-Tyr3-Octreotide PET in comparison to CT and bone scintigraphy. J Nucl Med 50:1214–1221
6. Kroiss A, Putzer D, Decristoforo C et al (2013) 68Ga-DOTA-TOC uptake in neuroendocrine tumour and healthy tissue: differentiation of physiological uptake and pathological processes in PET/CT. Eur J Nucl Med Mol Imaging 40:514–523
7. Prasad V, Baum RP (2010) Biodistribution of the Ga-68 labeled somatostatin analogue DOTA-NOC in patients with neuroendocrine tumors: characterization of uptake in normal organs and tumor lesions. Q J Nucl Med Mol Imaging 54:61–67
8. Ambrosini V, Nanni C, Zompatori M et al (2010) (68)Ga-DOTA-NOC PET/CT in comparison with CT for the detection of bone metastasis in patients with neuroendocrine tumours. Eur J Nucl Med Mol Imaging 37:722–727
9. Gabriel M, Decristoforo C, Kendler D et al (2007) 68Ga-DOTA-Tyr3-Octreotide PET in neuroendocrine tumors: comparison with somatostatin receptor scintigraphy and CT. J Nucl Med 48:508–518
10. Van Binnebeek S, Vanbilloen B, Baete K et al (2016) Comparison of diagnostic accuracy of 111In-pentetreotide SPECT and 68Ga-DOTATOC PET/CT: A lesion-by-lesion analysis in patients with metastatic neuroendocrine tumours. Eur Radiol 26:900–909

11. Slon V, Stein D, Cohen H et al (2015) Vertebral hemangiomas: their demographical characteristics, location along the spine and position within the vertebral body. Eur Spine J 24:2189–2195
12. Gaudino S, Martucci M, Colantonio R et al (2015) A systematic approach to vertebral hemangioma. Skeletal Radiol 44:25–36
13. Gilardi L, Vadrucci M, Grana CM (2017) Multiple vertebral hemangiomas: a potential pitfall in 68Ga-DOTATOC PET/CT interpretation. Endocrine 55:992–993
14. Skoura E, Alshammari A, Syed R et al (2015) Adolescent with 68Ga DOTATATE–avid vertebral hemangioma mimicking metastasis in PET imaging. Clin Nucl Med 40:e378–e379
15. Brogsitter C, Hofmockel T, Kotzerke J (2014) 68Ga DOTATATE uptake in vertebral hemangioma. Clin Nucl Med 39:462–463
16. Klinaki I, Al-Nahhas A, Soneji N, Win Z (2013) 68Ga DOTATATE PET/CT uptake in spinal lesions and MRI correlation on a patient with neuroendocrine tumor: potential pitfalls. Clin Nucl Med 38:e449–e453
17. Persaud T (2008) The Polka-dot sign. Radiology 246:980–981
18. Erlemann R (2006) Imaging and differential diagnosis of primary bone tumors and tumor-like lesions of the spine. Eur J Radiol 58:48–67
19. Balogova S, Talbot J-N, Nataf V et al (2013) 18F-fluorodihydroxyphenylalanine vs other radiopharmaceuticals for imaging neuroendocrine tumours according to their type. Eur J Nucl Med Mol Imaging 40:943–966
20. Thapa P, Ranade R, Ostwal V et al (2016) Performance of 177Lu-DOTATATE-based peptide receptor radionuclide therapy in metastatic gastroenteropancreatic neuroendocrine tumor: a multiparametric response evaluation correlating with primary tumor site, tumor proliferation index, and dual tracer imaging characteristics. Nucl Med Commun 37:1030–1037
21. Grillo F, Albertelli M, Brisigotti MP et al (2016) Grade increases in gastroenteropancreatic neuroendocrine tumor metastases compared to the primary tumor. Neuroendocrinology 103:452–459
22. Bucy PC (1929) The pathology of hemangioma of bone. Am J Pathol 5:381–388
23. Adams RL, Adams IP, Lindow SW et al (2005) Somatostatin receptors 2 and 5 are preferentially expressed in proliferating endothelium. Br J Cancer 92:1493–1498
24. Makhija M, Bofill ER (1988) Hemangioma, a rare cause of photopenic lesion on skeletal imaging. Clin Nucl Med 13:661–662
25. Jaimini A, D'Souza MM, Seniaray N et al (2016) Characterization of 'cold' vertebrae on 18F-FDG PET/CT. Nucl Med Commun 37:30–42
26. Domínguez M, Rayo J, Serrano J et al (2011) Vertebral hemangioma: 'Cold' vertebrae on bone scintigraphy and fluordeoxy-glucose positron emission tomography-computed tomography. Indian J Nucl Med 26:49–51
27. Savelli G, Perotti V, Rosso E et al (2016) 18F-fluorocholine PET/CT finding of a vertebral hemangioma. Clin Nucl Med 41:e390–e391
28. Nakayama M, Okizaki A, Ishitoya S, Aburano T (2012) 'Hot' vertebra on 18F-FDG PET scan: a case of vertebral hemangioma. Clin Nucl Med 37:1190–1193
29. Kazmierczak PM, Rominger A, Wenter V et al (2017) The added value of 68Ga-DOTA-TATE-PET to contrast-enhanced CT for primary site detection in CUP of neuroendocrine origin. Eur Radiol 27:1676–1684
30. Cives M, Rizzo F, Simone V et al (2016) Reviewing the osteotropism in neuroendocrine tumors: The role of epithelial-mesenchymal transition. Neuroendocrinology 103:321–334
31. Van Loon K, Zhang L, Keiser J et al (2015) Bone metastases and skeletal-related events from neuroendocrine tumors. Endocr Connect 4:9–17
32. Gauthé M, Richard-Molard M, Fayard J et al (2017) Prognostic impact of tumour burden assessed by metabolic tumour volume on FDG PET/CT in anal canal cancer. Eur J Nucl Med Mol Imaging 44:63–70
33. Dibble EH, Alvarez ACL, Truong M-T et al (2012) 18F-FDG metabolic tumor volume and total glycolytic activity of oral cavity and oropharyngeal squamous cell cancer: adding value to clinical staging. J Nucl Med 53:709–715
34. Riihimäki M, Hemminki A, Sundquist K et al (2016) The epidemiology of metastases in neuroendocrine tumors. Int J Cancer 139:2679–2686